Development of a miniature Stirling cryocooler for LWIR small satellite applications

Kirkconnell, C., Hon, R., Perella, M., Crittenden, T., Ghiaasiaan, S.

C. S. Kirkconnell, R. C. Hon, M. D. Perella, T. M. Crittenden, S. M. Ghiaasiaan, "Development of a miniature Stirling cryocooler for LWIR small satellite applications," Proc. SPIE 10180, Tri-Technology Device Refrigeration (TTDR) II, 1018002 (5 May 2017); doi: 10.1117/12.2259803

SPIE.

Event: SPIE Defense + Security, 2017, Anaheim, California, United States

Development of a miniature Stirling cryocooler for LWIR small satellite applications

C. S. Kirkconnell*[a], R. C. Hon[a], M. D. Perrella[b], T. M. Crittenden[b], S. M. Ghiaasiaan[b]
[a]West Coast Solutions, 6741 Brentwood DR, Huntington Beach, CA, USA 92648; [b]Georgia Institute of Technology, G.W. Woodruff School of Mechanical Engineering, Atlanta, GA, 30332

ABSTRACT

The optimum small satellite (SmallSat) cryocooler system must be extremely compact and lightweight, achieved in this paper by operating a linear cryocooler at a frequency of approximately 300 Hz. Operation at this frequency, which is well in excess of the 100-150 Hz reported in recent papers on related efforts, requires an evolution beyond the traditional Oxford-class, flexure-based methods of setting the mechanical resonance. A novel approach that optimizes the electromagnetic design and the mechanical design together to simultaneously achieve the required dynamic and thermodynamic performances is described. Since highly miniaturized pulse tube coolers are fundamentally ill-suited for the sub-80K temperature range of interest because the boundary layer losses inside the pulse tube become dominant at the associated very small pulse tube size, a moving displacer Stirling cryocooler architecture is used. Compact compressor mechanisms developed on a previous program are reused for this design, and they have been adapted to yield an extremely compact Stirling warm end motor mechanism. Supporting thermodynamic and electromagnetic analysis results are reported.

Keywords: SmallSat, Stirling, cryocooler, infrared, LWIR

1. INTRODUCTION

Present state of the art in electro-optical sensing for SmallSat platforms (less than 12U, i.e., < 0.012 m^3 stowed volume) is limited to uncooled technologies, such as visible wavelength and bolometer-type, low resolution long wave infrared (LWIR) sensors. Highly miniaturized cryocoolers that enable high resolution, intrinsic semiconductor infrared devices do not yet exist. High resolution infrared imaging has a tremendous range of applications, both looking into outer space and down at planetary bodies, as has been demonstrated on innumerable large spaceborne instruments. To fully exploit the utility of SmallSat technology, satellite providers must be able to offer miniaturized versions of these actively-cooled infrared sensors on these SmallSat platforms. In addition to using infrared SmallSats for these traditional missions, the growth of the satellite industry itself is creating new needs. As low Earth orbit (LEO) becomes more fully populated with small spacecraft performing more integrated and complex missions, high resolution mid wave infrared (MWIR) and LWIR imaging will become increasingly critical for robotic missions and space situational awareness (SSA). This is especially relevant considering the frequency of eclipses in LEO, i.e., absence of visible light during large portions of orbits when maneuvers and complex operations must inevitably be performed.

While miniature Joule-Thomson throttling cycle refrigeration remains an area of research interest, the focus of most recent studies is on linear cryocooler technology, encompassing both Stirling and pulse tube coolers, as offering the best near term potential to achieve highly miniaturized space cryocooling. For the reasons described herein, this particular research effort is focused on the development of a highly-miniaturized Stirling cryocooler to fill the aforementioned infrared SmallSat cryocooler technology gap.

The optimum SmallSat cryocooler (SSC) system must be extremely compact and lightweight, achieved herein by operating the cryocooler at a frequency of approximately 300 Hz. The present concept design is depicted in Figure 1. In addition to being small, efficient, and lightweight, the SSC must also be a “good neighbor” to the rest of the payload. Limited space and power budgets preclude the implementation of elaborate accommodation features for adverse effects. In the case of a cryocooler, this means that exported vibration and electromagnetic interference (EMI) effects must be minimized by design. Operating the SSC at high frequency greatly simplifies exported vibration mitigation by making passive damping techniques viable and compact while reducing the number of harmonics of concern for the optical payload. (Excitation above 500 Hz is generally beyond the range or concern for payload resonances, so it is highly likely that only the drive frequency and not the harmonics will require attenuation for the proposed SSC.) The most troublesome aspect of EMI for

*carlk@wecoso.com; phone 1 714 222-0424; fax 1 714 969-0049; wecoso.com

Tri-Technology Device Refrigeration (TTDR) II, edited by Richard I. Epstein, Bjørn F. Andresen, Tonny Benschop, Joseph P. Heremans, Sergey V. Riabzev, Mansoor Sheik-Bahae, Proc. of SPIE Vol. 10180, 1018002
 · doi: 10.1117/12.2259803

reciprocating cryocoolers is the 2X drive frequency current ripple imparted back onto the bus, a challenge also inherently mitigated by high frequency cryocooler operation.

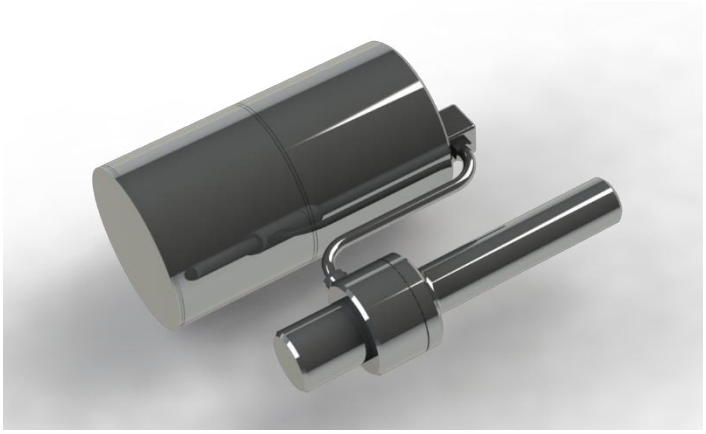

Figure 1. Solid model concept design for the SmallSat Stirling Cryocooler (SSC). Shown as a single-piston compressor with a "passive" Stirling expander (i.e., no expander motor). Overall size based upon thermodynamic modeling results presented herein. For reference, the length of the expander module is 2.5 cm as shown.

Operation at this frequency, which is well in excess of the 100-150 Hz characteristic of current state of the art, requires a radical improvement beyond traditional Oxford-class, flexure-based methods of setting mechanical resonance. The challenge is compounded in the present research because we have selected a Stirling cycle cryocooler for its inherent efficiency advantages, which brings with it the added complication of moving mechanisms in the expander as well as the compressor. This is in contrast to the pulse tube approach in which moving mechanisms are confined to the compressor. Additionally, advanced manufacturing techniques must be employed for joining dissimilar metals and to obtain the precision thermodynamic dimensions required for high efficiency, such as micron-scale feature dimensions in the heat exchanger matrices.

The focus of this paper is on the thermodynamic design of the SmallSat Cryocooler. Past research on 300 Hz class linear cryocoolers has focused primarily on pulse tube coolers, and in an even greater departure from the methods employed herein, thermoacoustically-driven coolers. Therefore, our initial efforts have been focused on the development of a thermodynamic design for a miniature Stirling cryocooler driven by a reciprocating linear motor compressor that addresses an operating point typical of what might be required for a SmallSat infrared imager, namely >200 mW @ 80K for less than 6 W DC input power to the electronics. Thermodynamic modeling has been performed using industry standard tools, namely Sage [1] and REGEN 3.3 [2]. The excellent agreement between the Sage and REGEN results is presented. The initial mechanical design concepts are presented, including the co-authors' earlier work on a highly representative ~250 Hz linear compressor. The paper concludes with planned next steps in the development, which include additional Sage optimization and computational fluid dynamics (CFD) modeling.

2. COMPARISON OF STIRLING AND PULSE TUBE APPROACHES

2.1 State of the Art Tactical Stirling Cryocoolers

In the size range of interest for the present effort, most of the commercial success to date has been achieved with miniature Stirling cryocoolers, such as the AIM Infrarot SX030 [3, Figure 2] and the Ricor K527 [4], both of which are linear coolers. (The high exported vibration and limited lifetime characteristics of rotary coolers make them unsuitable for the SmallSat IR missions of interest, in spite of their attractive compact size and mass, so they are not considered herein.) These and similar linear coolers from other tactical cryocooler manufactures, such as Thales Cryogenics [5], are primarily targeting High Operating Temperature (HOT) tactical infrared detector applications with cooling temperatures between 120K and 150K. While impressively compact with cryocooler mass <500g, these coolers are still oversized for SmallSat applicability. Furthermore, at the objective 80K LWIR operating temperature, even larger coolers are required, such as the

AIM SX040 [6]. The SX040 exceeds the target 200 mW @ 80K requirement, but it requires ~17 Wac and the compressor alone weighs 590g. The industry's focus on miniature Stirlings for the low end size and power range of the linear cooler market indicates the inherent superiority of the Stirling approach in this regime, yet the present state of the art does not support SmallSat mission requirements for the targeted temperature of 80K.

Figure 2. AIM SX-030 Cryocooler with passive balancer, a single-stage Stirling cryocooler driven by a single-piston compressor. Image provided courtesy of AIM Infrarot –Module GmbH.

2.2 Miniature Pulse Tube Coolers

Lockheed Martin is a recognized leader in miniature linear space cryocoolers. The performance and characteristics of these coolers as described in a recent publication are representative of present state of the art [7]. Also targeting the HOT IR market, the Lockheed "Microcryocooler," shown in Figure 3, is a single stage pulse tube driven by a dual opposed piston linear compressor. This cryocooler, based on the literature, appears to be a scaled-down Oxford flexure-suspension design operating in the range of ~100 Hz and weighing 310g (190g compressor, 120g coaxial pulse tube cold head – "standard" configuration). The Microcryocooler provides approximately 400mW cooling at 100K for 20 WAC input power to the compressor (i.e., electronics not included) at a rejection temperature of 300K.

Figure 3. Lockheed Martin Microcryocooler, a dual-opposed piston driven, co-axial pulse tube cryocooler. Image provided courtesy of Lockheed Martin Corporation.

2.3 Stirling – Pulse Tube Thermodynamic Comparison

High thermodynamic efficiency is essential for a small satellite cryocooler to meet the power and size requirements. Power to drive the cooler is at a premium because of the practical limits of how much solar panel can be stowed and deployed on the SmallSat bus, with 20 WDC total average power for an entire 3U satellite being a practical upper limit [8]. For the present effort, it has been assumed that the maximum power available for the cryocooler is 30% of the total, or only 6 WDC. Furthermore, high efficiency reduces the required input power for a given heat lift, which enables a smaller compressor motor, smaller swept volumes, and thus an overall reduction in size. Therefore, a comparison of the efficiency of the competing linear cooler architectures, Stirling and pulse tube, has been performed. This comparison would ideally

be performed at the objective 80K operating temperature, but the standard Microcryocooler in the relevant sub-20W input power class does not produce meaningful refrigeration at 80K. Therefore, the performances of the SX-030 and the Microcryocooler at 100K are compared.

Using the performance data from [7] as reported above, the Microcryocooler First and Second Law efficiencies are calculated as follows:

$$\beta_c = {}^{Tc}/_{(Th-Tc)} = {}^{100}/_{(300-100)} = 0.500$$

$$\beta = {}^{Qc}/_{Win} = {}^{0.40}/_{20} = 0.020$$

$$\beta_{II} = {}^{\beta}/_{\beta_c} = {}^{0.020}/_{0.500} = 0.040 = 4.0\%$$

Where *Tc* is the refrigeration temperature, *Th* is the rejection temperature, *Qc* is the net refrigeration load, *Win* is the AC power input to the cooler, β_c = the Carnot efficiency, β = thermodynamic (First Law) efficiency, and β_{II} = Second Law efficiency, i.e., the percentage of Carnot.

Using the SX-030 for comparison because of its close similarity in size (285g compressor v. 190g) to the Microcryocooler, a comparable data point from the SX-030 data sheet (175 mW @100K, 5 Win, 295K rejection temperature) shows that the Stirling is clearly more efficient, which supports the use of a Stirling for sub-100K SmallSat cryocooling:

$$\beta_c = {}^{100}/_{(295-100)} = 0.513$$

$$\beta = {}^{0.175}/_{5} = 0.035$$

$$\beta_{II} = {}^{0.035}/_{0.513} = 0.068 = 6.8\%$$

2.4 High Frequency Pulse Tubes

To our knowledge, no research on high frequency (>150 Hz) Stirling cryocoolers has been published, but impressive work has been published on pulse tubes operating in the 300 Hz regime. Zhu, et al. and Wang, et al., representing largely the same group of researchers from the Chinese Academy of Sciences, were able to achieve 1 W of cooling at 80K at an operating frequency of around 300 Hz using a thermoacoustic compressor for 1 kW of thermal input power, improving in efficiency by a factor of 2X in reducing the thermal input to 500 W in a second paper just two years later [9,10]. Although the pulse tube expanders are impressively small in this research, with pulse tube dimensions of 6 mm diameter x 40 mm length and regenerator dimensions of diameter of 10 mm x 30 mm length, the thermoacoustic compressor is very large, in fact several meters in length with a characteristic diameter of 50 mm. Clearly this architecture is not well suited to the SmallSat application in terms of size and power. This group's follow on work with a miniature coaxial pulse tube cooler driven by a linear compressor operating up to 280 Hz is more relevant to the present effort [11]. An interesting observation made by the authors is that the readily available 600# mesh stainless steel regenerator screen is "insufficient" for the purpose, an opinion with which we concur, and a motivation for our use of a micro-machined custom regenerator in the SSC. Reflective of the inherent challenge in achieving efficient operation at high frequency, the required compressor swept volume had to be increased to 11.6 cc to achieve resonance at 280 Hz. When compared to the < 0.1 cc swept volume of the SSC compressor, it is clear that this method of increasing resonance, evidently by increasing the stiffness of the pressure force, is also incompatible with the SmallSat objectives.

Ray Radebaugh's team at the National Institute of Science and Technology (NIST) and their collaborators have also been active in researching high frequency pulse tubes. Examples include work on a 120 Hz linear pulse tube cooler producing 3.35 W of cooling at 80K using a high capacity (up to 500W) pressure wave generator to demonstrate shorter cool down time [12, 13]. This research also showed that high pulse tube PV (pressure-volume) is achievable in pulse tubes operating at high frequency. More recent work describes operation up to 144 Hz using a compact Ricor K527 compressor to achieve 530 mW @ 120K [14]. Acoustic mismatch prevented effective operation below 100K in that test setup, and it is noted here that 100K has so far proven to be a difficult barrier to overcome for high frequency pulse tube coolers. (Computational fluid dynamics modeling is planned by the SSC team to investigate whether this is simply due to excessive boundary layer losses in these very small pulse tubes.)

3. THERMODYNAMIC MODELING

3.1 Modeling process

The software tools that were utilized in the thermodynamic analysis are REGEN 3.3 and Sage v11. These tools were applied in tandem and iteratively, using a methodology that has been successfully applied at Georgia Tech many times in the past [15, 16]. REGEN 3.3, developed and maintained by NIST, is an industry-standard 1-D finite difference model for the simulation of cryocooler regenerators. The design of a cold head starts with a rigorous design of the regenerator, followed by the sizing and characterization of other components using proven but purely empirical rules. Sage, also an industry-standard tool, is an object-oriented computer program which integrates modular 1D sub-models of each of the components found in typical cryocooler systems. Sage is capable of simulating a Stirling system in its entirety with relatively short computation time, and is therefore particularly suitable for optimization simulations. The Georgia Tech design methodology utilizes REGEN and Sage to determine the overall design of a cryocooler and to optimize the basic dimensions of the major components. These tools, however, are not capable of capturing the multi-dimensional flow losses that can sometimes have a severe impact on a cooler's performance. To address this, researches at Georgia Tech use computational fluid dynamics (CFD) simulations such as ANSYS Fluent to model the hydrodynamic behavior of detailed cooler components such as flow restrictions and orifices as part of their standard design approach. Past research by the SSC team [17] as well as others has proven that CFD simulations can predict the performance of linear coolers quite well. However, CFD simulations are computationally-intensive and therefore unsuitable for design/optimization purposes. Therefore, for this work, we focus on the upper-level design and optimization of the overall cryocooler system using only REGEN and Sage and leave detailed flow analysis and separate effects studies for later work.

3.2 REGEN analysis technique

REGEN 3.3 was used to model the fluid dynamics and heat transfer within the regenerator of the SSC. In REGEN other components such as the compression and expansion regions are not modeled directly, but indirectly through the application of appropriate boundary conditions at the inlet and outlet of the regenerator. REGEN accepts as user inputs the pressure ratio, mass flow rate, and mass flow-to-pressure phase angle at the cold end of the regenerator. Holding the physical dimensions of the regenerator constant, the porosity and cold-end mass flow were iteratively varied in order to maximize the regenerator's performance, defined by REGEN as the ratio of the net cooling power over the warm-end PV power input. REGEN results were used to provide target operating conditions for the system-level Sage model, which in turn provided updated boundary conditions to REGEN until the optimal regenerator design was determined.

The regenerator is of particular interest given its dominant impact on thermodynamic performance in linear coolers, including the SSC. In order to achieve the specified cooling and input power objectives, a parallel tube design, a standard design option in both REGEN and Sage, was selected using glass as the wall material. The parallel tube design allows for lower pressure drop across the regenerator compared with other porous filler materials such as screens and felts, while still providing adequate solid-to-gas heat transfer. The glass tube material helps to minimize heat leakage along the regenerator's axial direction due to its inherently low thermal conductivity. Preliminary optimization was performed to determine the optimum porosity and flow passage diameter as constrained by present state of the art in glass manufacturing, assumed here to be defined by a feature size limit of approximately 20 um.

3.3 Sage analysis technique

Using the REGEN results as the starting point, simulations were performed in Sage for comparison to REGEN to further verify the SSC concept. A highly simplified block diagram containing only the essential thermodynamic components of a Stirling cooler is shown in Figure 4. As the compressor oscillates the displacer is forced to cyclically compress and expand the gas at the warm and cold ends of the expander. The displacer phase angle, typically leading the compressor by ~70-90°, is set with a tuned spring-mass or motor (not shown) to achieve the desired phase angle and resonance at the drive frequency. For modeling convenience in the present study, the displacer piston has been replaced numerically with a stationary regenerator and actively-driven pistons at the warm and cold expander ends (Figure 5). The warm and cold end pistons oscillate in phase at the same swept volume to simulate the motion of a single piston. This simplifies the modeling and allows for faster and more flexible scoping analysis.

For the preliminary design optimization, simplified piston models were used which neglect seal leakage and frictional losses. Initial dimensions of the various components were chosen using REGEN 3.3 and experience-based empirical rules, and the total swept volumes and relative phase of the compressor and expander were optimized using Sage's built-in optimization tool to maximize the refrigeration at 80K. The modified regenerator design and operating conditions were

then re-modeled in REGEN 3.3 to verify agreement and provide confidence in the results. The optimized simulation at 80 K was selected as the baseline, yielding 400 mW cooling at 3.3W input PV power for this idealized case. The graphical representation of this simplified Sage model is shown in Figure 6.

Next, loss terms not considered in the idealized analysis were considered. As with any regenerator, axial conduction heat transfer through the porous regenerator material and the vessel walls play a significant role in reducing the total cooling power of the cryocooler. The porous regenerator filler material, in this case the glass tube bundle, might be wrapped in a cylindrical shell of smooth, low-conductivity plastic forming the displacer piston, sheathed within the cylindrical outer walls of the cooler which act as a pressure vessel. REGEN 3.3 only accounts for the axial conduction through the porous regenerator filler material itself but not the displacer or pressure vessel walls. As a conservative estimate, these conduction paths were added to the Sage model as a 0.005" (1.27E-4 m) thick cylindrical shell of low-conductivity PET plastic for the displacer wall and a 0.005" (1.27E-4 m) thick cylindrical shell of Inconel for the pressure vessel wall. The addition of these conduction paths reduced the total cooling power considerably to 216 mW at 80 K with 3.3 W input PV power. Considering that the original optimization was performed without these conduction losses considered, it is expected that future optimization iterations will result in a longer cold finger to regain some of this loss. This is discussed further later in the paper.

Continuing, also neglected by REGEN and the simplified Sage model are the seal leakage and shuttle losses of the displacer piston at the warm end of the regenerator. Replacing the simplified piston model in Sage with a rigorous shell-and-piston assembly with a 0.0015" (3.81E-5 m) radial gap further reduces the cooling power to 209 mW at 80 K with 3.8 W input power. A schematic of the rigorous Sage model is shown in Figure 7. Even with the addition of the conduction, seal, and shuttle losses, and without reoptimization, the SSC still provides 209 mW @ 80 K with < 3.8 W input PV power. Using nominal estimates of 70% for the motor efficiency and 90% for the drive electronics, the predicted input DC power is 6.0W, which is well within the available power budget on the targeted 3U spacecraft bus.

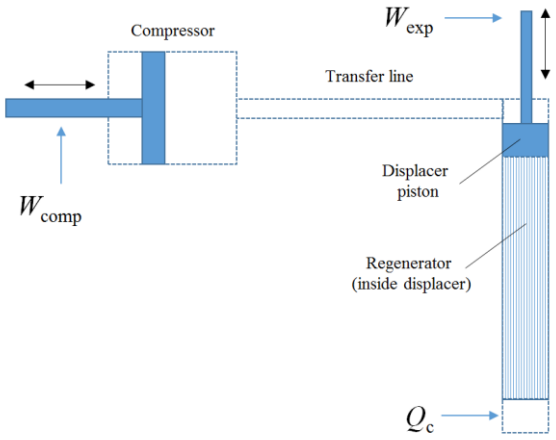

Figure 4. Basic Stirling cooler block diagram.

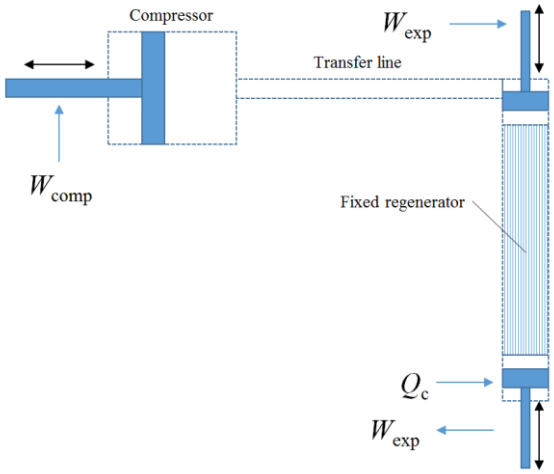

Figure 5. Simplified Sage model implementation.

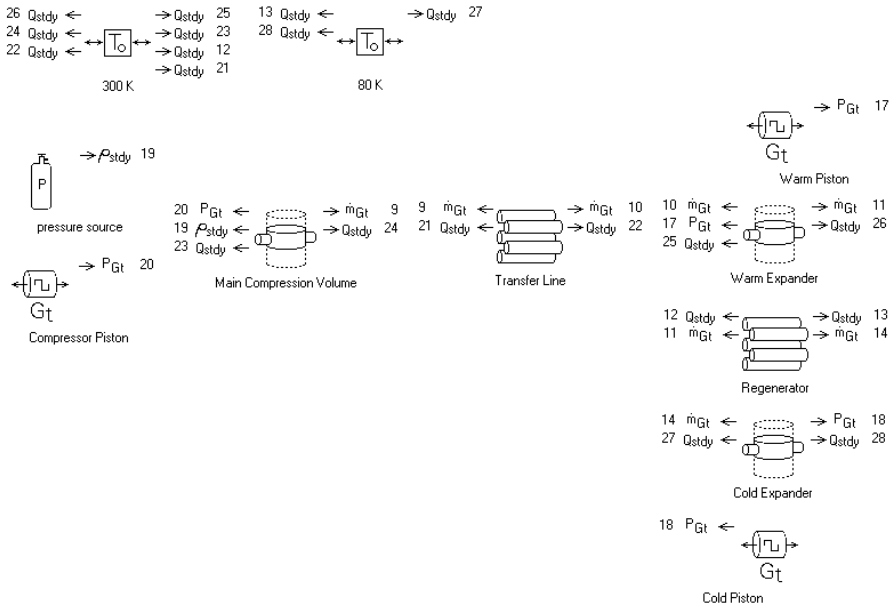

Figure 6. Simplified Sage model

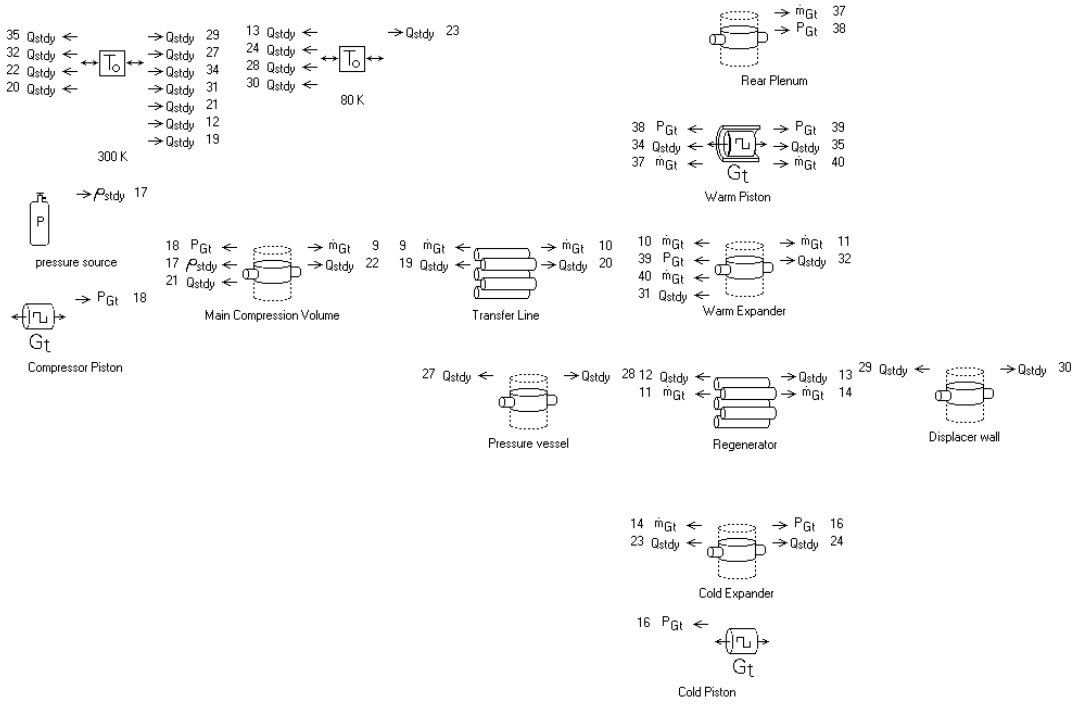

Figure 7. Rigorous Sage model

3.4 Comparison of REGEN and Sage results

The Sage and REGEN results were then compared over a wide range of cold tip temperature (50K to 150K) to assess modeling agreement and thereby enhance modeling confidence. In order to have accurate comparisons with REGEN, the simplified Sage model was used, which as previously discussed neglects the additional conduction, seal, and shuttle losses in the same way as REGEN. Because all of the heat absorbed by the cold finger must pass through the regenerator to be rejected, the cooling power of the regenerator provided by REGEN is used as the basis of comparison to the total cooling power of the system-level model in Sage.

The cold-end pressure ratio (PR) and mass flow-to-pressure phase angle ($\Phi_{m\text{-}p}$) from Sage were used as inputs for the REGEN simulations and are shown in Figure 8. The REGEN software iteratively varies the hot-end pressure and mass flow rate in order to match the target values provided as inputs. The hot-end pressure ratio and phase angle are computed and output by REGEN based on these inputs and are compared to the hot-end pressure ratio and phase angle from Sage in Figure 9. The figure shows excellent agreement between the two simulations in terms of the both pressure ratios and phase angles. Figure 10 shows the ratio of hot end mass flow rate to cold end mass flow rate for REGEN and Sage, once again showing excellent agreement, and Figure 11 compares the cooling power to PV input power for the entire temperature range in both simulations. These results provide high confidence in the thermodynamic modeling, particularly with respect to the regenerator.

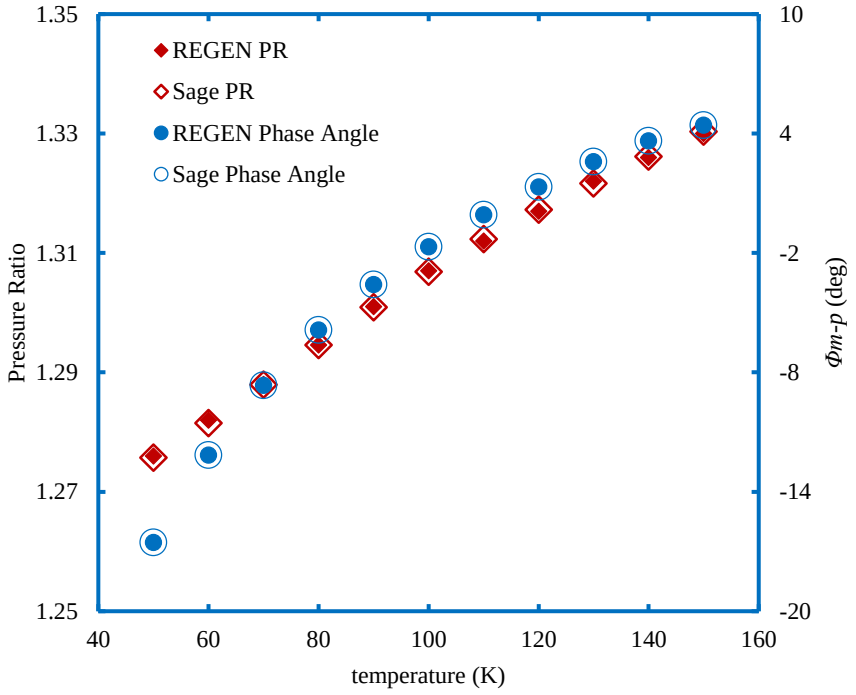

Figure 8. Cold-end Pressure Ratio and Phase Angle outputs from Sage used as inputs for REGEN simulations

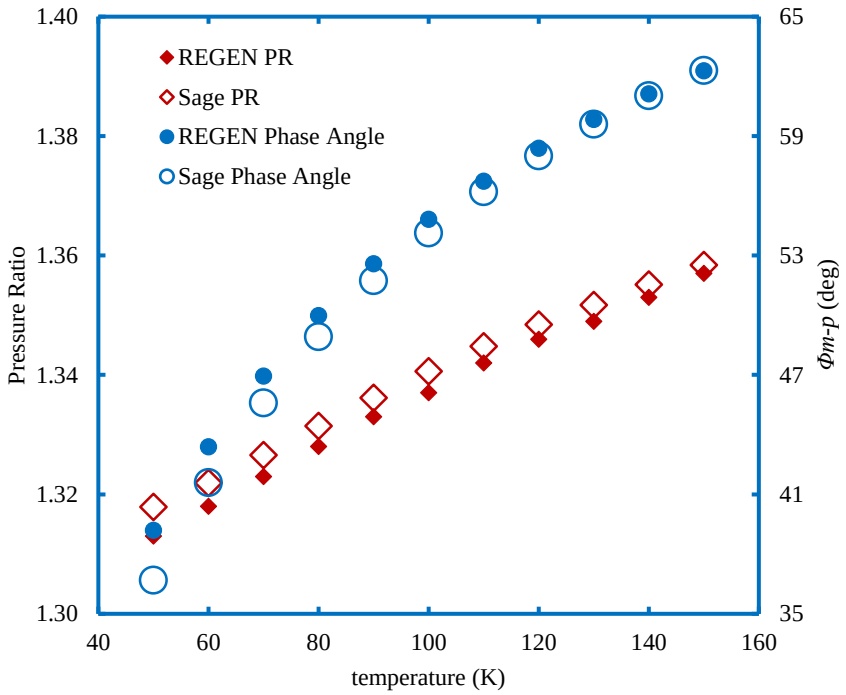

Figure 9. Warm-end Pressure Ratio and Phase Angle outputs from Sage and REGEN

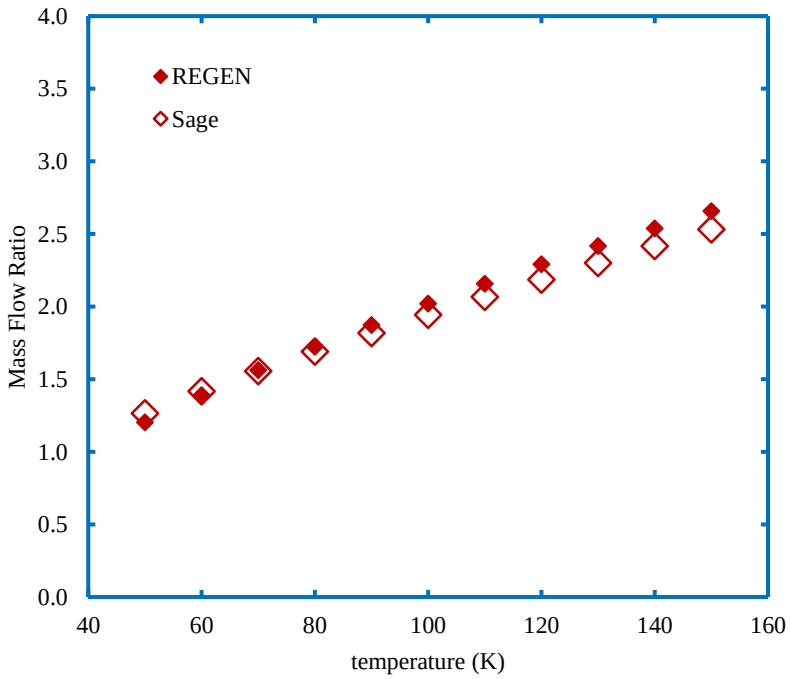

Figure 10. Ratio of Cold-end mass flow rate to Warm-end mass flow rate from Sage and Regen

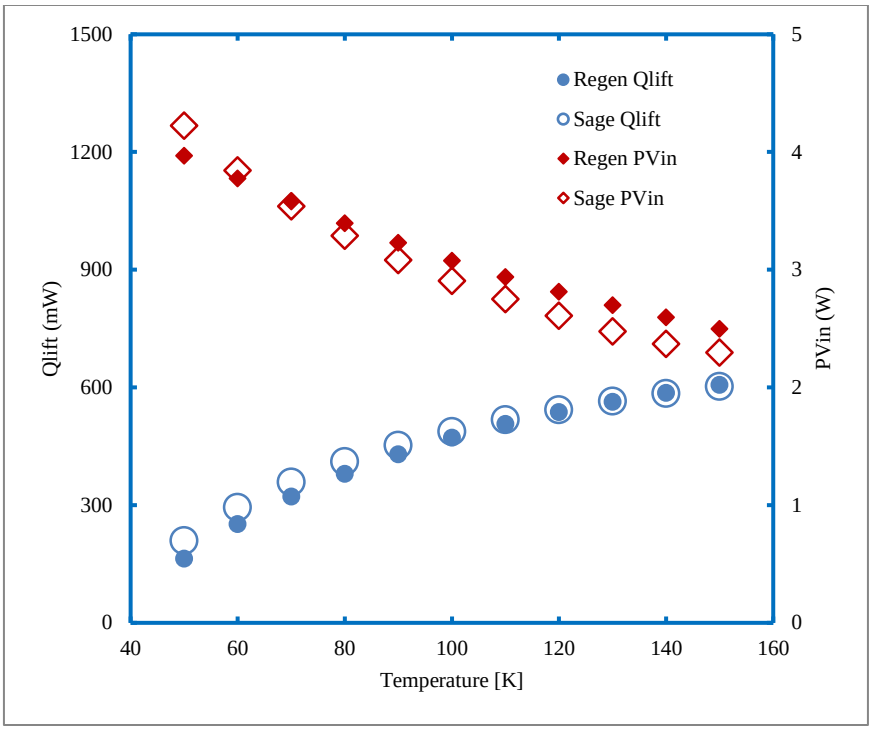

Figure 11. Comparison of cooling power (Qlift) and PV power input (PVin) from Sage and REGEN

4. MECHANICAL DESIGN

4.1 Compressor design

Under a previous program led by this same research team, a number of prototype compressors were designed, fabricated, and tested specifically with the aim of pairing them with a miniaturized pulse tube expander designed for high-frequency operation. A sample compressor prototype is shown in Figure 11, including a number of design elements (e.g., mechanical flanges for repeated assembly and disassembly) not required for a production version of the system. This particular unit featured an overall volume of 16.2 cm^3 and a weight of 67.8 grams (with models eliminating the experimental characterization features expected to attain a 10 cm^3 target volume and an estimated 50 gram weight). The initial design goals for the program targeted an operating frequency of 200 Hz, but further modeling suggested targeting frequencies near 300 Hz to provide better performance.

A sample result from the testing is shown in Figure 12, illustrating the frequency vs. displacement curve for a single excitation voltage. In this data, the charge spaces were left at atmospheric pressure levels with air as the working fluid to isolate the spring effects and resonance levels solely attributable to the mechanical design. The resonance frequency here is shown as between 240 and 250 Hz. Further testing with the addition of pressurized helium to the working space at a mean level of 2.0 MPa increased the resonance frequency to around 260 Hz, with greater frequency increases expected for greater working pressure levels and increased gas spring contributions. It is believed that with minimal adjustments, the core design used for this prototype can be modified to hit resonance at 300 Hz for the desired SSC working pressure.

When the compressor was operated at a filling pressure of 2.0 MPa, a pressure ratio of 1.17 was measured with a 10 W power input, which was lower than the target level and the calculated values which should be achieved for the measured displacement. It is believed that this discrepancy is due to the pressure measurement taking place in the transfer line rather than the compression space itself and is indicative of significant pressure losses at the exit of the compression space. Convolution in the gas passage exiting the compression space was the result of an innovative suspension system attempted with these prototypes which utilized a hardened, coated rod with precision jewel bearings at either end to maintain radial alignment. This approach was already proving problematic from an endurance standpoint to achieve infinite lifetime, as

some measure of wear was observed on the rod coatings under cyclic testing at 200 Hz with particulate contamination of the working fluid resulting. Although not fully demonstrated yet, early results suggest that using miniaturized flexure bearings for the suspension system would yield better results than the jewel bearing guide rod approach and eliminate all sliding surface contact from the design. Removing the need to pass the rod through the compression space would also simplify the fluid connection with expected improvements in the transmitted pressure ratio. It is expected that this approach and a few minimal design changes will allow this design to serve as a full production small-scale compressor capable of operating at 300 Hz and meeting all other necessary requirements.

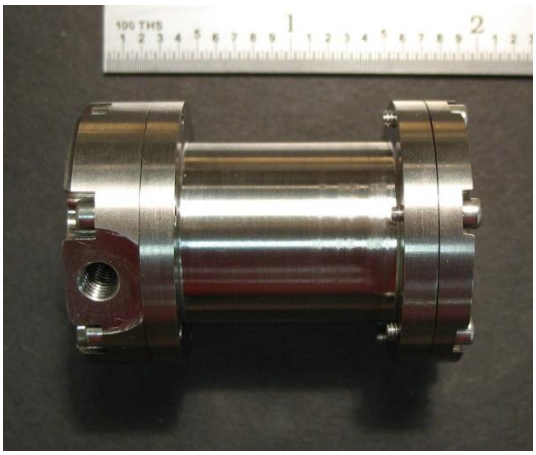

Figure 12. Flanged experimental compressor prototype allowing for easier assembly and disassembly.

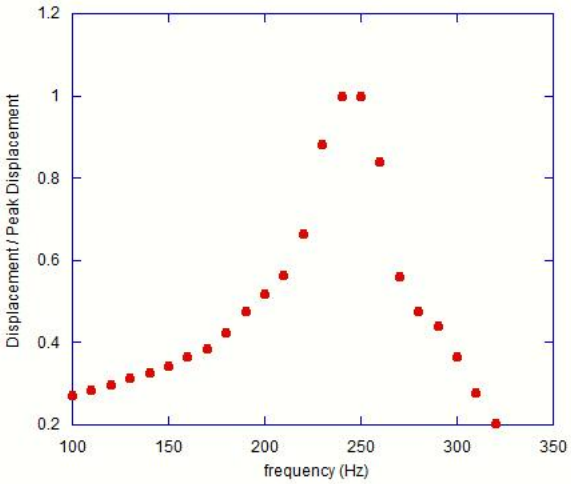

Figure 13. Displacement versus frequency curve for 12V pk-pk excitation voltage for prototype compressor (atmospheric pressure conditions)..

4.2 Expander design –warm end mechanism

As discussed in section 4.1, an earlier but related development program involved the design of a small scale cryocooler for relatively high temperature operation, and a Pulse Tube (PT) type expander was chosen as a result. Lower operating temperatures drive the current design away from the PT architecture, however an open trade exists as to whether this design will utilize a passive or active Stirling expander. Efficient operation of a Stirling cryocooler requires that the expander volume displacement amplitude and phase be carefully chosen. In a "passive" Stirling machine, these properties are set solely by the spring constant, mass, and damping characteristics of the expander mechanism itself. Alternatively,

a motor can be added to that same mechanism to yield an active Stirling machine. While the spring constant, mass and damping properties of an active Stirling expander mechanism still set the gross volume displacement and phase characteristics, motor force can be utilized by the system controller to tune those characteristics to their optimal thermodynamic values. The benefits of a passive machine are therefore mechanical and electrical simplicity, in addition to minimized package volume and mass. In contrast, active machines are characterized by the ability to achieve superior efficiency and capacity across a wide range of operating conditions.

It is worthwhile to note that efficiency is a prime consideration for SmallSat systems, as power generation and storage resources are severely limited. For instance, a typical 3U-sized system might be limited to 20W of total power, of which only a fraction is available for the cryocooler system itself. Waste heat rejection capability is similarly scarce, meaning that the introduction of a highly efficient cryocooler system provides a dual benefit: decreased power consumption in addition to reduced utilization of available heat rejection. While the reduced complexity, mass and volume associated with a passive design are clearly appealing for a miniaturized application, strong motivation exists to explore the implementation of an efficient active design - the additional mass and complexity can potentially be more than offset by system-level benefits.

A related consideration concerns the possibility that the SmallSat Stirling cryocooler will be particularly susceptible to high levels of unit-to-unit variation in terms of component mass and damping factors; manufacturing tolerances for the various relevant components are not expected to scale with the size of the component, nor do the values or repeatability of parasitics that contribute to the effective damping coefficient of the expander mechanism. Such variation can negatively impact the performance of a passive Stirling machine by moving the expander amplitude and phase away from optimal values, in which case there is little recourse but to implement costly and time-consuming unit-to-unit tuning and rework. In contrast, the motor of an active Stirling can be utilized to automatically compensate for this variation with no required mechanical rework. In a high production volume scenario, this is a significant advantage for the active design. The advantage carries over to the low production rate case of a single machine integrated into a single payload, as the temperatures and heat loads predicted via analysis at the beginning of a program often differ from the actual values when the payload is integrated or at the end of the payload's life. In this case, the ability to alter the Stirling expander volume displacement characteristics without making hardware changes is a distinct advantage for the active design. Such factors will play a significant role in the trade between passive and active designs for this SmallSat cryocooler.

As the trade between passive and active Stirling expander designs is performed, it is worth noting that the existing compressor electromagnetic design is directly applicable to the expander module. Its physically small, yet efficient and capable motor provides more than adequate ability to drive the Stirling expander piston to its optimal stroke length and phase, so long as the mechanism spring constant, mass and damping characteristics are reasonably close to their design values. If an active system is ultimately chosen, the ready availability of the warm-end electromagnetic design will significantly reduce development risk.

5. CONCLUSIONS AND FURTHER RESEARCH

Initial thermodynamic modeling has been completed for a highly miniaturized cryocooler operating at 300 Hz to achieve the objective small size required for use on small satellites cooling infrared sensor payloads operating as cold as 80 K. Modeling has been accomplished for this "SmallSat Stirling Cryocooler (SSC)" using two completely independent and proven software tools, REGEN and Sage, and excellent agreement has been demonstrated. This encouraging result indicates the suggested 300 Hz Stirling architecture is indeed viable. Past research efforts by this team have established the practicality of a resonant compressor design supporting the SSC frequency and size targets, providing further confidence. These compressor mechanism designs are presently being reoptimized for this application, including investigating an adaptation to yield the resonant mechanisms in the Stirling expander warm end.

The next phase of the research is underway. With the regenerator modeling confidence established, the full system Sage model with the secondary losses will be used to re-optimize the nominal thermodynamic design with the expectation that a somewhat longer cold finger will result from full consideration of all the conduction losses. Then, computational fluid dynamics (CFD) tools will be employed to investigate aspects of the design not readily amenable to inspection with the 1-D REGEN and control-volume based Sage tools. As the final thermodynamic sizing targets are achieved through these modeling efforts, detailed mechanical design to achieve the target geometries will commence. Incorporation of advanced

manufacturing techniques, in particular for the clearance seals, the regenerator, and the joining of dissimilar metals, poses the next major challenge for the SSC to become a viable spaceflight cryocooler.

REFERENCES

[1] http://sageofathens.com/
[2] http://math.nist.gov/archive/regen/
[3] http://www.aim-ir.com/fileadmin/files/Data_Sheets_Cooler/2014_neu/2014_AIM_SX030_engl.pdf
[4] http://www.ricor.com/products/split-linear/k527/
[5] Willems, D., Arts, R., de Jonge, G., Mullie, J., and Benschop, T., "Miniature Stirling Cryocoolers at Thales Cryogenics: Qualification Results and Integration Solutions," Cryocoolers 19, International Cryocooler Conference, Boulder, CO, 85-93 (2016).
[6] http://www.aim-ir.com/fileadmin/files/Data_Sheets_Cooler/Datasheet_SX040.pdf
[7] Nast, T., Olson, J. Champagne, P., Roth, E., Saito, E., Loung, V., McCay, B., Kenton, A., and Dobbins, C., "Development of Microcryocoolers for Space and Avionics Applications," Cryocoolers 19, International Cryocooler Conference, Boulder, CO, 65-74 (2016).
[8] Clark, C., "Huge Power Demand … Itsy-Bitsy Satellite: Solving the CubeSat Power Paradox," Proceedings of the 24th Annual AIAA/USU Conference on Small Satellites, ref. SSC10-III-5 (2010), http://digitalcommons.usu.edu/cgi/viewcontent.cgi?article=1202&context=smallsat
[9] Zhu, S.L., Yu, G.Y., Dai, W., Luo, E.C., Wu, Z.H., and Zhang, X.D., "Characterization of a 300 Hz Thermoacoustically-driven Pulse Tube Cooler," *Cryogenics*, vol. 49, 51-54 (2009).
[10] Wang, X., Yu, G., Dai, W., Luo, E., and Zhou, Y., "Influence of Acoustic Pressure Amplifier Tube on a 300 Hz Thermoacoustically Driven Pulse Tube Cooler," Journal of Applied Physics, vol. 108, 074905-1 to -5 (2010).
[11] Wang, X., Yu, L., Zhu, J., Yu, G., Dai, W., Hu, J., Luo, E., Li, H., "A Miniature Coaxial Pulse Tube Cooler Operating above 100 Hz," Cryocoolers 17, International Cryocooler Conference, Boulder, CO, 107-114 (2012).
[12] Vanapalli, S., Lewis, M., Gan, Z. Radebaugh, R., "120 Hz Pulse Tube Cryocooler for Fast Cooldown to 50K," Applied Physics Letter, vol. 90, 072504-1 to -3 (2007).
[13] Vanapalli, S., Lewis, M., Grossman, G., Gan, Z. Radebaugh, R., ter Brake, H.J.M. "Modeling and Experiments on Fast Cooldown of a 120 Hz Pulse Tube Cryocooler," *Advances in Cryogenic Engineering*, vol. 53, 1429-1436 (2008).
[14] Radebaugh, R., Garaway, I., and Veprik, A., "Development of Miniature, High Frequency Pulse Tube Cryocoolers," Infrared Technology and Applications XXXVI, Proc. Of the SPIE, vol. 7660, 2J (2010).
[15] Pathak, M., Periodic Flow Physics in Porous Media of Regenerative Cryocoolers, PhD Thesis, Georgia Institute of Technology (2013).
[16] Mulcahey, T.I., Convective Instability of Oscillatory Flow in Pulse Tube Cryocoolers Due to Asymmetric Gravitational Body Force, PhD Thesis, Georgia Institute of Technology (2014).
[17] Cha, J.S., Ghiaasiaan, S.M., Desai, P.V., Harvey, J.P., and Kirkconnell, C.S., "Multi-Dimensional Effects in Pulse Tube Refrigerator", *Cryogenics*, 658-665 (2006).